

Quantum field theory in the Schrödinger picture

Peter Gerwinski

Bochum University of Applied Sciences, Campus Velbert/Heiligenhaus,
Kettwiger Straße 20, 42579 Heiligenhaus, Germany

(Dated: 11 May 2022)

The many-particle Schrödinger equation of quantum electrodynamics is set up and solved numerically, using a generalised version of a method from quantum chaos. The results for pair annihilation and creation are qualitatively correct. This is an alternative method for second quantisation, which works in the Schrödinger picture, without using time-ordered perturbation theory (Feynman diagrams). It is thus, by construction, compatible with general relativity and with noncommutative geometry via the spin connection.

I. INTRODUCTION

The most precise description of nature currently provided by theoretical physics consists of general relativity and quantum field theory. Perturbative methods based on time-ordered products, in particular Feynman diagrams, have proven extremely successful for studying the Standard Model of quantum field theory. Applying the same methods to general relativity leads to nonrenormalisable divergences.

The most well-known approaches to overcome this problem are string theory [1] and loop quantum gravity [2]. To date there is, however, no experimental evidence for either of these theories [3, §2C]. Both approaches have in common that they apply established quantisation methods, path integrals or canonical quantisation, to gravity, predicting quantum effects of spacetime itself such as a granularity at the Planck scale. In both theories it is still an open problem how to recover general relativity.

Another approach is to treat gravity as a classical field together with unmodified quantum field theory. These *semiclassical* approaches predict quantum phenomena which include gravity, such as Hawking radiation [4] and effects of gravity on the quantum mechanics of macroscopic objects, which might be in range of experimental tests, soon [5].

A promising alternative approach is to change the prescription for second quantisation in such a way that it “interpolates” between perturbatively quantised general relativity at low energies and gravity as a classical field at high energies [6].

A very different approach is noncommutative geometry [7–12]. It unifies all fundamental forces of physics by ascribing them to gravity on a non-commutative spacetime with discrete extra dimensions. It does not address the nonrenormalisable divergences which arise from applying the established perturbative quantisation methods to gravity. Instead it successfully uses the methods of general relativity to study the foundations of quantum field theory. The main point of criticism of noncommutative geometry is that no quantisation procedure compatible with this framework has been found so far [11]. (Another problem concerning the predicted mass of the Higgs boson has been cleared up [12].)

In this work we develop a non-perturbative method to

quantise fermionic and bosonic fields in such a way that they remain compatible with general relativity and with noncommutative geometry via the spin connection.

Working in the Schrödinger picture, we extend the methods of mathematical physics from the one-particle Dirac equation [13, §§ 28.4–28.5] to many-particle quantum electrodynamics. To solve the resulting hyperbolic partial differential equation numerically we develop an explicit algorithm with adaptive stepsize. This numerical method is a generalisation of established methods known from the field of quantum chaos [14–18].

Methods of this type are commonly applied to single-particle quantum wave functions and to classical fields, including general relativity. In this work, we successfully apply such a method to simulate pair annihilation and creation in quantum fields.

II. QUANTUM ELECTRODYNAMICS – THE SCHRÖDINGER PICTURE

We start from the well-known Lagrangian density of quantum electrodynamics,

$$\mathcal{L} = \bar{\psi}(i\hbar c\gamma^\mu \partial_\mu - q\gamma^\mu A_\mu - mc^2)\psi - \frac{1}{4}F_{\mu\nu}F^{\mu\nu}. \quad (1)$$

By keeping c , \hbar and the coupling constant q (charge) as variables instead of setting them to 1 we leave the door open for studying the limits $c \rightarrow \infty$ and $\hbar \rightarrow 0$.

We derive the Hamiltonian density,

$$\mathcal{H} = \bar{\psi}(mc^2 - i\hbar c\gamma^j \partial_j)\psi + \frac{1}{4}F_{\mu\nu}F^{\mu\nu} - \bar{\psi}q\gamma^\mu A_\mu\psi, \quad (2)$$

and substitute the time-independent field operators

$$\hat{\psi}(x) = \int d^3p \sum_{\sigma=0}^3 \psi_{p,\sigma} c_{p,\sigma} e^{-\frac{i}{\hbar}px}, \quad (3)$$

$$\hat{\bar{\psi}}(x) = \int d^3p \sum_{\sigma=0}^3 c_{p,\sigma}^+ \bar{\psi}_{p,\sigma} e^{\frac{i}{\hbar}px}, \quad (4)$$

$$\hat{A}_\mu(x) = \int d^3k \sqrt{\frac{\hbar c^2}{2\omega_k}} \left(a_{k,\mu} e^{ikx} + a_{k,\mu}^+ e^{-ikx} \right) \quad (5)$$

for the wave functions $\bar{\psi}$, ψ (fermions), and A_μ (photons).

For $\sigma \in \{0, 1\}$, the normalised amplitude vectors $\psi_{p,\sigma}$ and their Dirac adjoints $\bar{\psi}_{p,\sigma} = \gamma^0 \psi_{p,\sigma}^*$ describe eigenstates with positive energy (particles). For $\sigma \in \{2, 3\}$

they describe eigenstates with negative energy (anti-particles).

The fermion ladder operators $c_{p,\sigma}$ and $c_{p,\sigma}^+$ are kept generic for now and will be reinterpreted later to separate particles and anti-particles,

$$c_{p,\sigma} = b_{p,\sigma}, \quad c_{p,\sigma}^+ = b_{p,\sigma}^+ \quad \text{for } \sigma \in \{0, 1\}, \quad (6)$$

$$c_{p,\sigma} = d_{-p,\sigma}^+, \quad c_{p,\sigma}^+ = d_{-p,\sigma} \quad \text{for } \sigma \in \{2, 3\}. \quad (7)$$

The photonic ladder operators $a_{k,\mu}$ and $a_{k,\mu}^+$ correspond to the μ^{th} component of a plane wave of the electromagnetic four-potential with wave vector k .

Following the customary path of quantum electrodynamics, we separate $e^{-\frac{i}{\hbar} p x}$ from the momentum eigenstates, recombine them, carry out the integrals over x and p' , and obtain the Hamiltonian

$$H = \int d^3x \mathcal{H}(x) = H_\psi + H_A + H_J \quad (8)$$

which consists of the Hamiltonian of free fermions

$$H_\psi = \int d^3p \sum_{\sigma=0}^3 c_{p,\sigma}^+ \bar{\psi}_{p,\sigma} (mc^2 - i\hbar c \gamma^j \partial_j) \psi_{p,\sigma} c_{p,\sigma}, \quad (9)$$

the Hamiltonian of free photons,

$$H_A = \int d^3k \sum_{\mu=0}^3 \frac{1}{2} \hbar \omega_k (a_{k,\mu}^+ a_{k,\mu} + a_{k,\mu} a_{k,\mu}^+), \quad (10)$$

where $\omega_k = c|k|$, and the interaction Hamiltonian

$$H_J = -qc \int d^3p \int d^3k \sum_{\mu=0}^3 \sqrt{\frac{\hbar c^2}{2\omega_k}} (a_{k,\mu} + a_{-k,\mu}^+) \sum_{\sigma=0}^3 \sum_{\sigma'=0}^3 c_{p-\hbar k,\sigma'}^+ \bar{\psi}_{p-\hbar k,\sigma'} \gamma^\mu c_{p,\sigma} \psi_{p,\sigma}. \quad (11)$$

In the free Hamiltonians H_ψ and H_A the ladder operators combine to particle number operators, which are diagonal in momentum representation and do not cause any serious trouble. The non-perturbative treatment of the interaction Hamiltonian H_J while taking account of fermions and anti-fermions is nontrivial and will be the main topic of this paper.

A. Dynamics of the Fermions

Our Schrödinger equation

$$i\hbar \frac{\partial}{\partial t} \Psi(t) = H\Psi(t) \quad (12)$$

has the formal solution

$$\Psi(t + \Delta t) = \exp\left(-\frac{i}{\hbar} \int_t^{t+\Delta t} H dt'\right) \Psi(t), \quad (13)$$

where $\Psi(t)$ denotes the combined wave function of the fermions and the photons.

In momentum representation, the free Hamiltonians H_ψ and H_A can be described by diagonal matrices. The interaction Hamiltonian H_J contains a coupling between the fermions and the photons, so we can treat it as a linear operator only in the approximation of small time intervals Δt . In other words, we calculate the time development of the fermions under the influence of the stationary photons, and vice versa. Then the double integral of H_J makes it a fully-occupied matrix in momentum representation.

Instead of expanding the exponential into a power series, we proceed by writing the operator inside the exponential in its eigenbasis, so we can carry out the exponential without approximation. With a fully-occupied matrix such as H_J this is only in reach of current computers when the total number of basis states involved does not exceed a few thousands. In the field of quantum chaos, this has successfully been applied to bound systems whose Hilbert space is finite-dimensional, for example the kicked top [14, 16–18]. When we want to simulate systems which correspond to experiments in quantum field theory, in particular scattering systems, we need to consider a larger number of eigenstates.

In the following we generalise a method used in the field of quantum chaos for non-relativistic single-particle scattering systems [15] to quantum field theory.

The approximation of small time intervals Δt allows us to replace the integral by a multiplication and to neglect the non-commutativity of the ingredients of H ,

$$e^{-\frac{i}{\hbar} H \Delta t} = e^{-\frac{i}{\hbar} H_\psi \Delta t} e^{-\frac{i}{\hbar} H_A \Delta t} e^{-\frac{i}{\hbar} H_J \Delta t} + \mathcal{O}(\Delta t^2). \quad (14)$$

This approximation can be improved to higher orders of Δt ; see [19] for details.

The Hamiltonian H_ψ of free fermions is diagonal in momentum representation. Together with the γ^0 from the Dirac adjoint $\bar{\psi}_{p,\sigma}$ we write it as a matrix over spinor space for each momentum p ,

$$H_\psi(p) := \gamma^0 mc^2 - \sum_{j=1}^3 c \gamma^0 \gamma^j p_j. \quad (15)$$

When we store the fermionic wave functions in momentum representation and decompose them, at each momentum p , into eigenstates of $H_\psi(p)$, we can apply $e^{-\frac{i}{\hbar} H_\psi \Delta t}$ to the wave functions without further approximation.

Essentially the same is possible for H_J in position representation, but it requires some preparation.

As the first step, we apply a reverse Fourier transform to H_J from momentum to position representation. This turns the double integral over p and k , a convolution, into a single integral over x ,

$$H_J = -(2\pi)^{\frac{3}{2}} qc \int d^3p \sum_{\sigma'=0}^3 \sum_{\sigma=0}^3 c_{p,\sigma'}^+ \bar{\psi}_{p,\sigma'} \mathcal{F} \left(\sum_{\mu=0}^3 \gamma^\mu (a_{x,\mu} + a_{x,\mu}^+) \psi_{x,\sigma} c_{x,\sigma} \right) (p), \quad (16)$$

where \mathcal{F} denotes the Fourier transformation, and

$$a_{x,\mu} = \mathcal{F}^{-1} \left(\sqrt{\frac{\hbar c^2}{2\omega_k}} a_{k,\mu} \right) (x), \quad (17)$$

$$\psi_{x,\sigma} c_{x,\sigma} = \mathcal{F}^{-1} (\psi_{-p,\sigma} c_{-p,\sigma}) (x). \quad (18)$$

The actual interaction is now diagonal in position representation. Thus it makes sense to speak of the interaction at a specific position x , preserving causality.

While we deal with the fermions, we replace all photonic ladder operators $a_{k,\mu}, a_{k,\mu}^\dagger$ by their expectation values $A_\mu(k), A_\mu^*(k)$ in the current state of the system, the electromagnetic field. As will be shown later, this approximation is surprisingly accurate.

Although we have switched from momentum to position representation, the indices σ and σ' of the fermionic ladder operators $c_{x,\sigma}$ and $c_{x,\sigma'}^\dagger$ still refer to momentum eigenstates. It is tempting to carry out the sums over σ and σ' to make the ladder operators together with the momentum eigenstates sum up to a unity operator. We do not do that because we will still need them later to distinguish between particles ($\sigma \in \{0, 1\}$) and anti-particles ($\sigma \in \{2, 3\}$).

At a given position x the electromagnetic field and the Dirac matrices form a Hermitian matrix $A(x)$ in spinor space which has the same structure as the momentum operator, again together with the γ^0 from $\bar{\psi}_{x,\sigma'}$,

$$A(x) := \sum_{\mu=0}^3 (A_\mu(x) + A_\mu^*(x)) \gamma^0 \gamma^\mu. \quad (19)$$

We decompose the fermionic wave function – in a given momentum eigenstate σ , but in position representation and at a given position x – into the eigenstates of $A(x)$, so we can directly apply the exponential.

The result is no longer a momentum eigenstate, but we can decompose it into momentum eigenstates σ' after we have Fourier transformed the wave functions back to momentum representation.

B. Fermions and Anti-Fermions

It is the recomposition into particle and anti-particle states, which implements pair annihilation and pair creation. To make this obvious, we revisit the interaction Hamiltonian H_J in momentum representation and write it as

$$H_J = -qc \int d^3p' \sum_{\sigma'=0}^3 \int d^3p \sum_{\sigma=0}^3 c_{p',\sigma'}^\dagger \bar{\psi}_{p',\sigma'} A(p' - p) \psi_{p,\sigma} c_{p,\sigma} \quad (20)$$

with the interaction matrix

$$A(\hbar k) = \sum_{\mu=0}^3 \sqrt{\frac{\hbar c^2}{2\omega_k}} (a_{k,\mu} + a_{-k,\mu}^\dagger) \gamma^\mu. \quad (21)$$

The interaction Hamiltonian H_J contains the operator $c_{p',\sigma'}^\dagger c_{p,\sigma}$, which maps the momentum eigenstate

$\psi_{p,\sigma}$ to the momentum eigenstate $\psi_{p',\sigma'}$. It also contains $c_{p,\sigma}^\dagger c_{p',\sigma'}$, which does the opposite. Thus the restriction of H_J to the two-state subspace of the momentum eigenstates $\psi_{p,\sigma}$ and $\psi_{p',\sigma'}$ can be written using

$$c_{p',\sigma'}^\dagger c_{p,\sigma} + c_{p,\sigma}^\dagger c_{p',\sigma'} = \begin{pmatrix} 0 & 1 \\ 1 & 0 \end{pmatrix}. \quad (22)$$

When we denote the two components of our wave function in this subspace by

$$\psi_0(t) := \langle \psi_{p,\sigma} | \Psi(t) \rangle, \quad (23)$$

$$\psi_1(t) := \langle \psi_{p',\sigma'} | \Psi(t) \rangle, \quad (24)$$

the interaction part of a time step of length Δt in the solution of our Schrödinger equation in this subspace reads, up to $\mathcal{O}(\Delta t^2)$,

$$\begin{aligned} \begin{pmatrix} \psi_1(t + \Delta t) \\ \psi_0(t + \Delta t) \end{pmatrix} &= e^{-\frac{i}{\hbar} H_J \Delta t} \psi \begin{pmatrix} \psi_1(t) \\ \psi_0(t) \end{pmatrix} \\ &= \exp \left(iC \begin{pmatrix} 0 & 1 \\ 1 & 0 \end{pmatrix} \right) \begin{pmatrix} \psi_1(t) \\ \psi_0(t) \end{pmatrix} \\ &= \begin{pmatrix} \cos C \psi_1(t) + i \sin C \psi_0(t) \\ \cos C \psi_0(t) + i \sin C \psi_1(t) \end{pmatrix}, \end{aligned} \quad (25)$$

where

$$C := -\frac{q}{\hbar} \Delta t A(p' - p). \quad (26)$$

So the interaction manifests as a complex “rotation” between two fermionic eigenstates.

In the case where both fermionic eigenstates $\psi_{p,\sigma}$ and $\psi_{p',\sigma'}$ denote (anti-) particles, eq. (25) describes the transition between two states of the (anti-) particle with different momenta and different spins resulting from emission or absorption of photons with momentum $\hbar k = p' - p$.

In the other case one eigenstate belongs to a particle and the other one to an anti-particle. Then we must reinterpret the ladder operators according to Feynman-Stückelberg.

Let $\psi_{p,\sigma}$ describe a particle and $\psi_{p',\sigma'}$ an anti-particle. Then $c_{p,\sigma} = b_{p,\sigma}$ remains an annihilation operator for a particle, but the creation operator becomes another annihilation operator for a spacetime-mirrored anti-particle, $c_{p',\sigma'}^\dagger = d_{-p',\sigma'}$. Likewise, $c_{p,\sigma}^\dagger = b_{p,\sigma}^\dagger$ and $c_{p',\sigma'} = d_{-p',\sigma'}^\dagger$. Their combination $c_{p',\sigma'}^\dagger c_{p,\sigma} = d_{-p',\sigma'} b_{p,\sigma}$ maps the two-particle state to the vacuum state.

Now we reverse the roles of p,σ and p',σ' . Then $\psi_{p,\sigma}$ describes an anti-particle and $\psi_{p',\sigma'}$ a particle, and the combined operator $c_{p',\sigma'}^\dagger c_{p,\sigma} = b_{p',\sigma'}^\dagger d_{-p,\sigma}^\dagger$ maps the vacuum state to the two-particle state.

Again H_J contains both combinations. We write their sum as

$$d_{-p',\sigma'} b_{p,\sigma} + b_{p,\sigma}^\dagger d_{-p',\sigma'}^\dagger = \begin{pmatrix} 0 & 1 \\ 1 & 0 \end{pmatrix}. \quad (27)$$

Equation (25) applies without change, but now it rotates between the vacuum state and the two-particle state. Depending on which one of both states is occupied, this case describes both pair annihilation and pair creation.

When we perform calculations and simulations with these wave functions, we represent the anti-particles as “Dirac holes”, i. e. as *CPT*-reversed vacuum wave functions. There are several methods to implement this. Special care must be taken when decomposing and recombining two fermionic wave functions in momentum representation, one of which is *CPT*-reversed. Again see [19] for details.

As a side note, this reaffirms that the “Dirac sea” approach, which is also used in noncommutative geometry [10], is equivalent to the Feynman-Stückelberg interpretation.

In summary, we can compute the effect of the time development operator $e^{-\frac{i}{\hbar}H\Delta t}$ on the fermions as follows.

- The fermions are stored as two spinor-valued wave functions. One represents the particles. The other one stores the anti-particles as *Dirac holes*.
- At each momentum p , we decompose the fermionic wave functions into eigenstates of $H_\psi(p)$ and apply the free time evolution operator $e^{-\frac{i}{\hbar}H_\psi(p)\Delta t}$ to them, taking into account that the wave function of the anti-particles is *CPT*-reversed.
- We switch from momentum to position representation by applying reverse Fourier transforms to all wave functions.
- At each position x , we decompose the fermionic wave functions into eigenstates of the interaction matrix $A(x)$ and apply the the time evolution operator of the interaction, $e^{-\frac{i}{\hbar}H_J\Delta t}$.
- We switch back to momentum representation by applying Fourier transforms to all wave functions.
- We decompose the resulting fermionic wave functions into momentum eigenstates and recombine them into wave functions of particles and of anti-particles.

By iterating this procedure we can calculate the time development of the fermions under the influence of the photons. As mentioned above, this first-order method can be generalised to higher orders of Δt .

C. Dynamics of the Photons

The time development operator for the interaction of the photons can be written as

$$e^{-\frac{i}{\hbar}H_J\Delta t} = \exp\left(\int d^3k \sum_{\mu=0}^3 \alpha_\mu(k) a_{k,\mu}^+ - \alpha_\mu^*(k) a_{k,\mu}\right), \quad (28)$$

where

$$\alpha_\mu(k) = \frac{i}{\hbar}qc\Delta t \int d^3p \sum_{\sigma=0}^3 \sum_{\sigma'=0}^3 \bar{\psi}_{p+\hbar k,\sigma'} \gamma^\mu \psi_{p,\sigma} c_{p+\hbar k,\sigma'}^+ c_{p,\sigma}. \quad (29)$$

This is a displacement operator for coherent states in momentum representation, which means that the time development operator for photons under the influence of fermions maps a coherent state to another coherent state.

When a coherent state evolves freely in time, it remains a coherent state. Together with eq. (28) this implies that we can simulate the full dynamics of a realistic field of photons by storing them as a field of coherent states, provided that the initial state of the photons is a coherent state itself. This holds, for instance, for the vacuum state.

A coherent state with parameter $\alpha_{k,\mu}$ is an eigenstate of the matching annihilation operator $a_{k,\mu}$. Thus our approximation in subsection II A, where we substituted all photonic ladder operators with their expectation values in the current state of the photons, is in fact exact.

The integral over p is a convolution which can be calculated using Fourier transforms from momentum to position representation and back. Thus the actual interaction takes place in position representation, where it acts locally rather than over a distance, and causality is maintained.

III. NUMERICAL RESULTS

As we have seen above, the “natural” way to describe a many-particle system of fermions and photons in the Schrödinger picture consists of two spinor-valued wave functions for the fermions and the anti-fermions, plus a field of coherent states for the photons. To simulate the time development of such a system in a computer we store all three wave functions point-wise.

Due to limitations of computer memory and calculation performance we restrict ourselves to two spatial dimensions.

By applying the steps described above iteratively we can simulate the time development of an initial state. This method is similar to the explicit Euler method of first order in Δt . It can be improved to higher orders of Δt , and we can implement time-step control. See [19] for details.

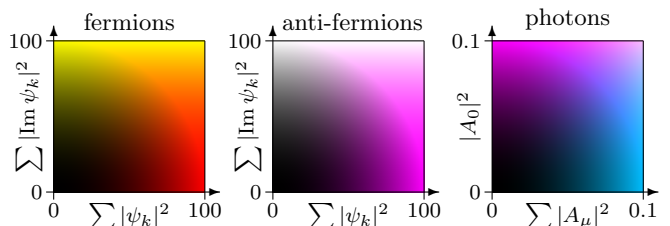


Figure 1. Pair annihilation: colour scheme for Fig. 2–4. For the fermions and anti-fermions, one colour dimension (green) is the sum of the squares of the imaginary parts of the spinor components, and the other one (red or magenta) is the norm of the spinor. For the photons, one colour dimension (red) is the absolute square of the zero-component, and the other one (cyan) is the norm of the four-vector.

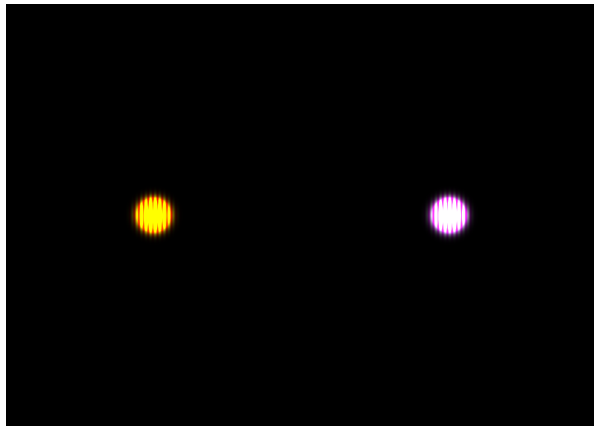


Figure 2. Pair annihilation: initial state. The wave function of the fermions (left) is shown in yellow. The red lines indicate regions with a small imaginary part and are thus perpendicular to the mean momentum vector. Likewise, the wave function of the anti-fermions (right) is shown in white and magenta. See the text for a discussion of the units.

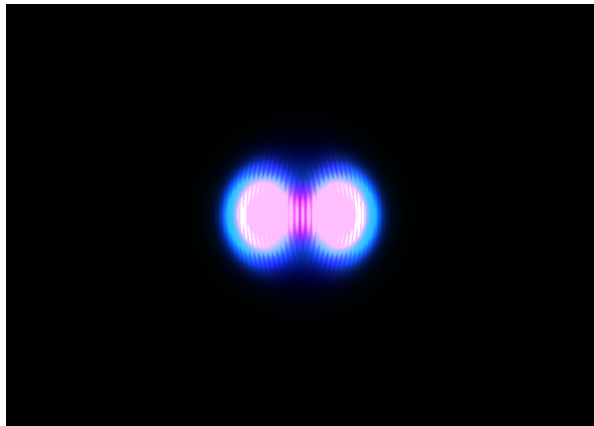


Figure 3. Pair annihilation: shortly after the collision, $t = 2.26$. (See the text for a discussion of the units.) The fermions and anti-fermions have annihilated parts of each other and generated photons, shown in rose and cyan.

The numeric computation of the Fourier transforms on a discretised space [20] induces periodic boundary conditions. To avoid interference of the outgoing photonic wave function with itself we can either make the spatial window so big that the wave function cannot reach the boundary, or absorb it numerically before it does.

We do not simulate the electrostatic fields generated by the fermions because they would make the wave packets dissolve out of numerical visibility before they collide. We suppose that this problem can be solved by increasing the spatial window of the simulation, which would require more computing resources.

In the following simulations we visualise the wave functions of the fermions and anti-fermions (spinors) and of the photons (coherent states, four-vectors) using the colour scheme depicted in Fig. 1.

To simulate pair annihilation, we prepare wave func-

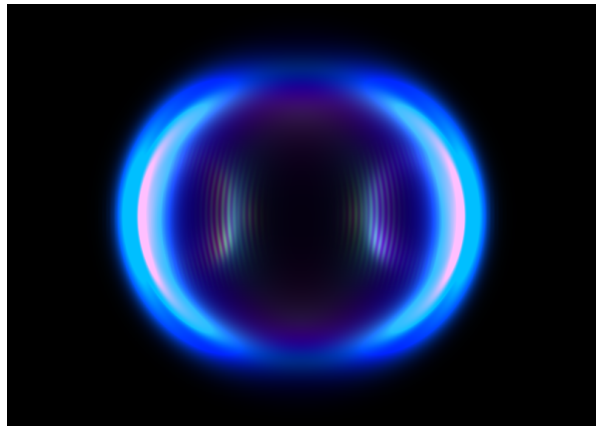


Figure 4. Pair annihilation: outgoing wave functions, $t = 3.00$. In addition to the outgoing photons there are also small remainders of the fermions and anti-fermions, which have been reflected or transmitted rather than annihilated.

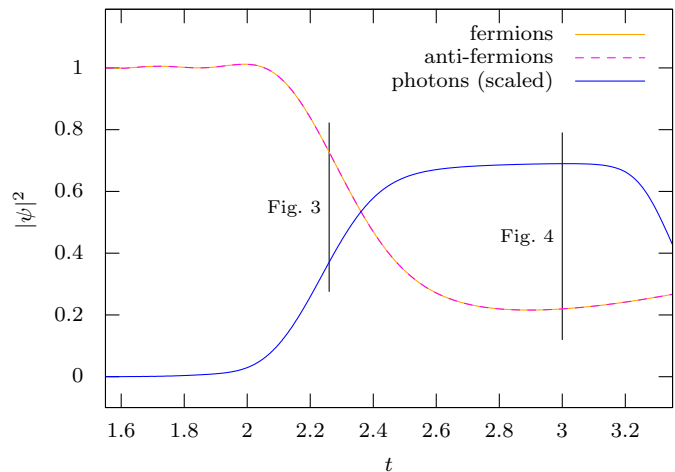


Figure 5. Pair annihilation: norm of the wave functions, scaled by a factor of 30 for the photons. (See the text for a discussion of the time unit.)

tions of fermions and anti-fermions as Gaussian wave packets as shown in Fig. 2. Their mean positions are separated; their mean momenta are chosen such that they will collide.

The simulation works with dimensionless numerical parameters for \hbar , c , and the fermion masses and charges. When we specialise for electrons and positrons, the time unit is 0.19 attoseconds, and the space unit corresponds to a distance of about 1.16 Ångström between the centres of the two wave packets in the initial state. (See [19] for further details.)

Figure 3 shows the state of the simulation after several iterations. The wave packets of the fermions and anti-fermions have collided and already annihilated parts of each other, generating arc-shaped photonic wave functions.

Figure 4 shows the outgoing wave functions after the collision. The norms of the fermionic wave functions have

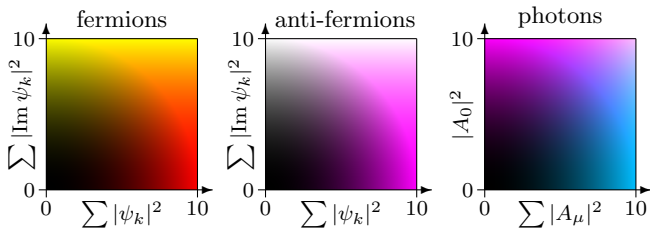


Figure 6. Pair creation: colour scheme for Fig. 7–9. Same as for pair annihilation (Fig. 1), but scaled differently.



Figure 7. Pair creation: initial state. Two colliding photonic wave packets are shown in cyan and blue. Two additional stationary fermionic wave packets in the centre have negligible norms and are almost invisible. (Again, see the text for a discussion of the units.)

shrunk significantly, leaving behind an outgoing photonic wave function.

Figure 5 shows the time development of the norm of the wave functions. During the pair annihilation the norm of the fermionic wave functions shrinks to less than one quarter of its initial value, which means that the probability for annihilation is over 75 % in this scenario. The norm of the photonic wave function grows. The increase of the norm of the fermions after $t \gtrsim 2.7$ and its small oscillations for $t \lesssim 2$ are due to pair creation. The decrease of the norm of the photons after $t \gtrsim 3.2$ is due to their absorption at the border of the spatial window of the simulation.

To simulate pair creation, we prepare wave functions of two colliding photonic wave packets, plus wave functions of fermions and anti-fermions with zero momentum and negligible norm in the centre. (If we initialised the fermionic wave functions to exact vacuum states, they would remain in that state even if the vacuum state becomes unstable.) In the visualisation we use the same colour scheme, but with a different scale, see Fig. 6.

Figure 7 visualises the initial state. In this simulation the time unit is 0.13 attoseconds, and the space unit corresponds to a distance of about 0.77 Ångström between the centres of the two wave packets in the initial state.

The photonic wave packets propagate and get arc-

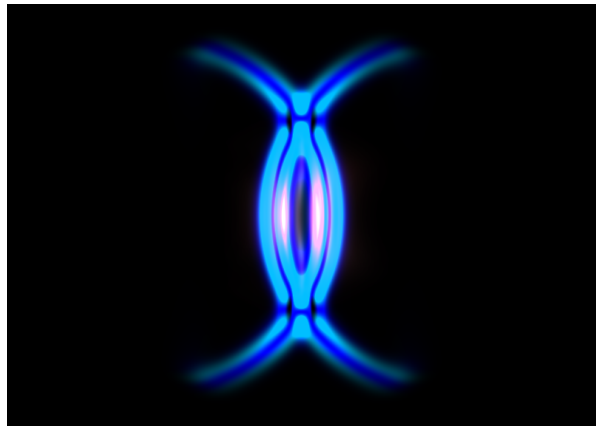


Figure 8. Pair creation: shortly after the collision, $t = 1.17$. In the regions which were exposed to overlapping photonic wave functions the norm of the fermionic wave packets has increased.

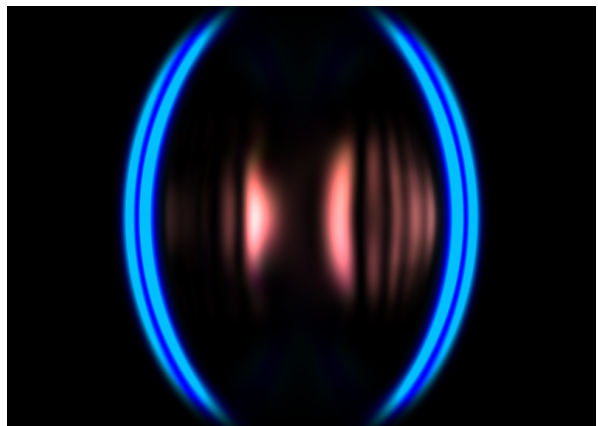


Figure 9. Pair creation: outgoing wave functions, $t = 2.10$. The outgoing photons are being absorbed at the border of the spatial window of the simulation, leaving behind wave packets of fermions and anti-fermions with small momenta.

shaped. Where they overlap they leave behind regions where the norm of the fermionic wave functions got increased, see Fig. 8 and 9. Figure 10 shows the norm of the wave functions in the case of pair creation. The oscillations of the fermionic wave functions between $t \approx 0.8$ and $t \approx 1.6$ are due to interference between the two photonic wave packets. The slight decrease of the fermionic wave functions after $t \gtrsim 1.6$ is due to annihilation of the newly created pairs. The asymmetry is due to limited numerical precision.

These simulations of pair annihilation and creation are qualitatively correct. In contrast to the well-established perturbative methods they were simulated in a framework whose extension to general relativity is straightforward, but was not thought to be suitable for studying quantum field theory so far.

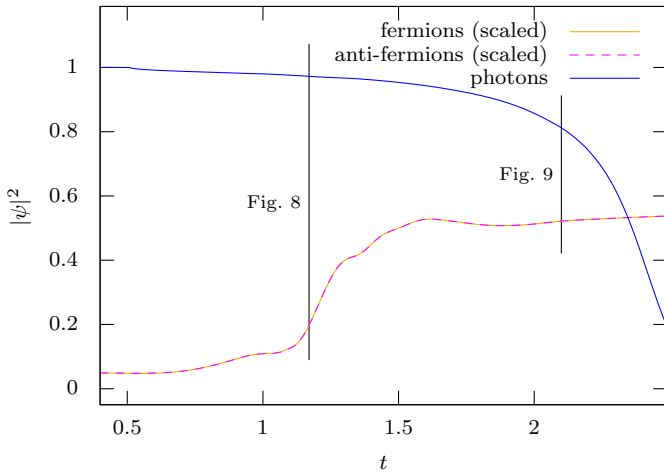


Figure 10. Pair creation: norm of the wave functions, scaled by a factor of 5 for the fermions. (See the text for a discussion of the time unit.)

IV. CONCLUSIONS AND OUTLOOK

The incompatibility between general relativity and quantum field theory consists of nonrenormalisable divergences, which arise from applying time-ordered per-

turbation theory to gravity.

The approach developed in this paper does the opposite. It applies the main tool of general relativity, solving a partial differential equation, to quantum electrodynamics, the simplest case of quantum field theory. It successfully simulates effects of second quantisation, pair annihilation and creation, without using time-ordered perturbation theory and without producing singularities.

The extension of this method from quantum electrodynamics to the full Standard Model might require significantly more computational power, depending on the transferability of the concept of coherent states from the photons to the other bosons. To include general relativity we have to apply the spin connection to incorporate curvature of spacetime, and we have to use the many-particle wave functions as sources for the Einstein field equations. All this is expected to be laborious, but straightforward.

In conclusion we have developed an alternative method for second quantisation, which is compatible with gravity and with noncommutative geometry.

ACKNOWLEDGMENTS

I am very grateful to Herbert Schmidt and to Karol Życzkowski for fruitful discussions which significantly improved this paper.

-
- [1] E. Witten: *What every physicist should know about string theory*. *Physics Today* **68** (11), 38 (2015).
- [2] C. Rovelli: *Quantum Gravity*. Cambridge Monographs on Mathematical Physics (Cambridge University Press, 2004), ISBN 0-521-83733-2.
- [3] C. Rovelli: *Loop Quantum Gravity*. *Living Rev. Rel.* **1**, 1 (1998). [arXiv:gr-qc/9710008](https://arxiv.org/abs/gr-qc/9710008).
- [4] S. Giddings, W. Nelson: *Quantum emission from two-dimensional black holes*. *Phys. Rev. D* **46**, 2486 (1992). [arXiv:hep-th/9204072](https://arxiv.org/abs/hep-th/9204072).
- [5] H. Yang ,H. Miao, D. Lee, B. Helou, Y. Chen: *Macroscopic Quantum Mechanics in a Classical Spacetime*. *Phys. Rev. Lett.* **110**, 170401 (2013). [arXiv:1210.0457](https://arxiv.org/abs/1210.0457).
- [6] S. Hossenfelder: *A possibility to solve the problems with quantizing gravity*. *Phys. Lett. B* **725** (4-5) 473 (2013). [arXiv:1208.5874](https://arxiv.org/abs/1208.5874).
- [7] A. H. Chamseddine, A. Connes: *The Spectral Action Principle*. *Commun. Math. Phys.* **186**, 731–750 (1997). [arXiv:hep-th/9606001](https://arxiv.org/abs/hep-th/9606001).
- [8] A. Connes, M. Marcolli: *Noncommutative Geometry, Quantum Fields and Motives*. *Am. Math. Soc. Coll. Publ.* **55** (2008). ISBN 978-0-8218-4210-2.
- [9] T. Schücker: *Forces from Connes’ Geometry*. *Lect. Notes Phys.* **659**, 285–350 (2005). [arXiv:hep-th/0111236](https://arxiv.org/abs/hep-th/0111236)
- [10] T. Schücker: *Spin Group and Almost Commutative Geometry* (2000). [arXiv:hep-th/0007047](https://arxiv.org/abs/hep-th/0007047).
- [11] J. Aastrup, J. Møller Grimstrup: *Intersecting Connes Noncommutative Geometry with Quantum Gravity* (2006). [arXiv:hep-th/0601127](https://arxiv.org/abs/hep-th/0601127).
- [12] A. H. Chamseddine, A. Connes: *Resilience of the Spectral Standard Model*. *JHEP* **1209** 104 (2012). [arXiv:1208.1030v2](https://arxiv.org/abs/1208.1030v2).
- [13] H. Triebel: *Analysis und mathematische Physik*. 2. Auflage, Leipzig 1984, VLN 294-375/23/84. English edition: *Analysis and mathematical physics*. Dordrecht 1986, ISBN 90-277-2077-0.
- [14] F. Haake: *Quantum signatures of chaos*. 3rd edition, Berlin-Heidelberg 2010, ISBN 978-3-642-05427-3.
- [15] P. Gerwinski, P. Šeba: *Quantum resonances due to classical stability islands*. *Phys. Rev. E* **50** 3615–3622 (1994).
- [16] P. Gerwinski, F. Haake, M. Kuš, H. Wiedemann, K. Życzkowski: *Semiclassical spectra without periodic orbits for a kicked top*. *Phys. Rev. Lett.* **74** 1562–1565 (1995).
- [17] P. A. Braun, P. Gerwinski, F. Haake, H. Schomerus: *Semiclassics of rotation and torsion*. *Z. Phys. B* **100** 115–127 (1996).
- [18] P. Gerwinski, F. Haake: *Semiclassical Floquet spectra without periodic orbits from ħ-expansion of Floquet matrix*. *Lecture Notes in Physics* **485**, 112–121 (1997).
- [19] P. Gerwinski: *Quantum Field Theory. A New Approach, Compatible with Gravity* (2021). <https://www.peter.gerwinski.de/phys/qft-approach.pdf>
- [20] M. Frigo, S. G. Johnson: *The design and implementation of FFTW3*. *Proc. IEEE* **93** (2), 216–231 (2005).

Contact: peter.gerwinski@hs-bochum.de
<https://www.peter.gerwinski.de/physics/>
 License: CC BY-SA 4 or later